HAL
archives-ouvertes.fr

Facial animation with wrinkles

Marie-Luce Viaud, Hussein Yahia

▶ **To cite this version:**

Marie-Luce Viaud, Hussein Yahia. Facial animation with wrinkles. [Research Report] RR-1753, INRIA. 1992. inria-00076993

HAL Id: inria-00076993
https://hal.inria.fr/inria-00076993

Submitted on 29 May 2006

HAL is a multi-disciplinary open access archive for the deposit and dissemination of scientific research documents, whether they are published or not. The documents may come from teaching and research institutions in France or abroad, or from public or private research centers.

L'archive ouverte pluridisciplinaire **HAL**, est destinée au dépôt et à la diffusion de documents scientifiques de niveau recherche, publiés ou non, émanant des établissements d'enseignement et de recherche français ou étrangers, des laboratoires publics ou privés.

UNITÉ DE RECHERCHE
INRIA-ROCQUENCOURT

Institut National
de Recherche
en Informatique
et en Automatique

Domaine de Voluceau
Rocquencourt
B.P. 105
78153 Le Chesnay Cedex
France
Tél.:(1) 39 63 55 11

Rapports de Recherche

1992

25ème anniversaire

N° 1753

Programme 4
Robotique, Image et Vision

FACIAL ANIMATION WITH WRINKLES

Marie-Luce VIAUD
Hussein YAHIA

Septembre 1992

RR_1753

Un Systeme d'Animation Faciale Integrant une Modelisation des Rides d'Expression

Marie-Luce Viaud , *Hussein Yahia*
Inria-Rocquencourt
B.P. 105, 78153 Le Chesnay Cedex, France
e-mail luce@bora.inria.fr
hussein@bora.inria.fr

Abstract

We propose a 3D facial animation system in which expressive wrinkles are taken into account and integrated into the process of facial animation. Starting from a reference wrinkle mask in which isolines are aligned with potentially existing expressive wrinkles, we present some techniques for editing the mask and for optimizing transfering the reference mask to another face. We present a user-friendly modeling system to animate the forces associated with the muscles of the face. Then we describe the geometrical modeling of expressive wrinkles and their implementation during motion control.

Résumé

Ce rapport présente un système d'animation faciale 3D dans lequel les rides d'expression sont modélisées et animées. Nous commencons par définir un masque de référence sur lequel toutes les rides d'expressions sont éditées et alignées avec les isolignes de la surface. Nous proposons ensuite diverses techniques pour editer le masque et transferer des attributs d'un masque vers un autre visage. Le système présenté ici, developpé en C dans le modeleur ACTION 3D, a été concu afin d'offrir un maximum d'interactivité à l'utilisateur. En particulier l'animation des forces qui creent les rides est particulièrement simple. Nous présentons donc la modélisation géométrique des rides d'expression et leur implementation en vue de la phase d'animation et de production.

Facial Animation with Wrinkles

Marie-Luce Viaud , *Hussein Yahia*
Inria-Rocquencourt
B.P. 105, 78153 Le Chesnay Cedex, France
e-mail luce@bora.inria.fr
hussein@bora.inria.fr

Abstract

We propose a 3D facial animation system in which expressive wrinkles are taken into account and integrated into the process of facial animation. Starting from a reference wrinkle mask in which isolines are aligned with potentially existing expressive wrinkles, we present some techniques for editing the mask and for optimizing transfering the reference mask to another face. We present a user-friendly modeling system to animate the forces associated with the muscles of the face. Then we describe the geometrical modeling of expressive wrinkles and their implementation during motion control.

CR Categories and subject descriptors: Computer Graphics, Three Dimensional Graphics and Realism-Animation, Computer Graphics, Computational Geometry and Object Modelling, Curve, surface, solid and object representation.

Additional Keywords: Deformable Mechanics, Energy Minimization, Interaction, Expressive Wrinkles, Facial Animation.

1 Introduction.

Facial Animation is a part of 3D Character Animation concerned with the modeling, motion control and rendering of human faces. The reader is refered to [Kl89], [Pa82, Pa74, Pa89], [Di89], [LePa89], [Tha88], [PlaBa81], [Wa87], [KuAr90], [NaHuRiDo90], [Wi90] to get an idea of the significant work done on that subject.

We present in this paper a facial animation system in which we tried to solve some remaining problems of 3D facial animation. We propose a system in which expressive wrinkles are geometrically modeled and combined with the forces used to simulate the action of muscles. This is done by integrating the skin's elasticity into the process of animation. We present a system which has been made as user-friendly as possible, and we propose some methods to help the user copy facial attributes from one face to another.

2 What are wrinkles ?

Human beings become increasingly marked as they grow old. Whereas outer signs of aging appear over the entire body, our faces are the primary target of time's work, and one major sign of aging is the appearance and persistence of wrinkles. Wrinkles are an important factor of human mimicry: understanding and interpreting facial expressions depends (among other things) on their amplitude and frequency. One can differentiate two types of wrinkles: expressive wrinkles and microwrinkles due to aging. Expressive wrinkles are present at all ages, even on babies, but become permanently visible from approximately age 30 . Their appearance comes from, among other things, the microscopic transformations of the hypodermal layer over time. Indeed, elastic connective fibers of the hypodermal layer are stretched and become thiner. Collagen fibers gather themselves in sheaves. leaving the skin tissue less homogeneous, particularly at those points much affected by muscles tension and compression. Epidermis cells regenerate themselves at a slower rate, and tend to favor a specific orientation, thus creating microfurrows.

These two phenomena generate the two most important characteristics of wrinkles: appearance of the microfurrow which draws the wrinkle, and appearance of the bulge of the wrinkle . Furthermore, the dermo-epidermic junction (the boundary between epidermis and dermis) unfolds itself, considerably changing the skin's elasticity. These three actions strongly modify the skin's response under the action of muscles.

Expressive wrinkles are creases generated by the action of muscles on the skin tissue. Indeed, facial muscles * possess one origin (connecting to the skeleton) and an insertion point connecting to deep fascia tissue. The skin is stretched and compressed directly by the tension of the muscles exactly at the insertion point. As the skin's elasticity varies over time, these creases vary accordingly. Observation shows that their amplitude varies, but not their shape and number: wrinkles may appear at peripheral points or extend themselves, but main creases remain unchanged. Hence we can associate with each muscle a deformation function and a description of the creases it may potentially generate.

Although wrinkles vary from one face to another, they can be described in uniform manner. We thus define a typical and flexible wrinkle mask, which will be refered as to the "reference mask" in what follows. We will explain in the next section how to generate a wrinkle mask for a given face from the reference mask.

3 Generation of a 3D wrinkled face

Starting from an atlas of all existing expressive wrinkles [Hj69], we make a Cardinal spline surface [Cl81] in which 0-isolines † are aligned with all existing wrinkles. It should be noticed that this reference mask is generated at a given scale, allowing the possibility of adding new wrinkles. The reference mask is depicted in figure 1 .

*The reader is refered to [RoDe91] for a complete description of facial muscles.

†If $(u, v) \rightarrow \phi(u, v)$ is a parameterization of a spline patch, a v_0 - *isoline* is a curve $u \rightarrow \phi(u, v_0)$ for a fixed v_0. In the same way a u_0 - *isoline* is a curve $v \rightarrow \phi(u_0, v)$. By 0-isolines we mean the two curves corresponding to $u_0 = 0$ and $v_0 = 0$.

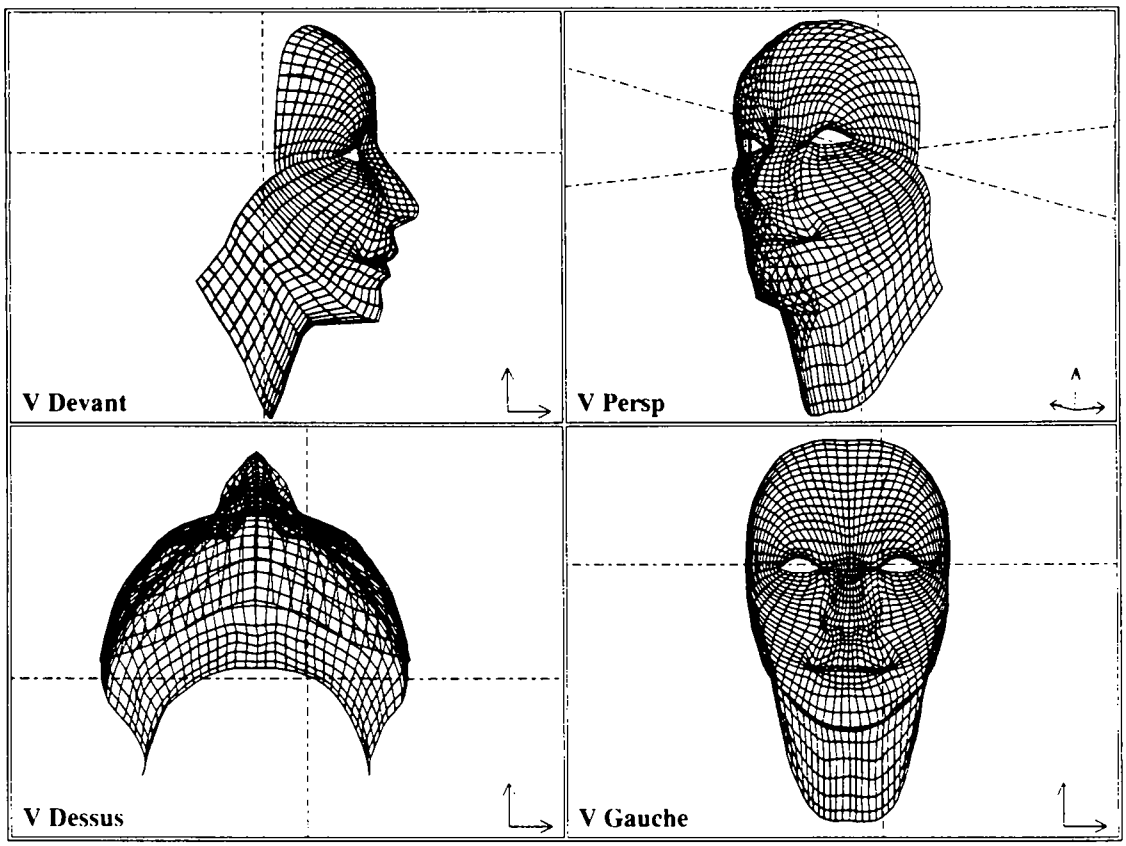

Fig. 1: The reference wrinkle mask

3.1 Flattening a mask

A mask is projected cylindrically and the cylinder is flattened to get a 2D mask. We need to choose a cylinder for which the mapping from the mask to the cylinder will have as little distortion as possible. To do so, a cylinder is characterized by its direction vector $\vec{d}$, its radius r and an origin G (see figure 2). We want to find r, G and $\vec{d}$ which minimize a certain energy related to the mapping error distortion.

One coordinate of $\vec{d}$ is fixed by an appropriate initial choice: the user must provide an initial cylinder not orthogonal to the desired one. Suppose this coordinate is $z = Z_0$. Let $\vec{d} = \begin{pmatrix} \alpha \\ \beta \\ Z_0 \end{pmatrix}$ and $g = \begin{pmatrix} x \\ y \\ z \end{pmatrix}$, where coordinates are defined relative to a fixed orthogonal frame $(O, \vec{i}, \vec{j}, \vec{k})$. We

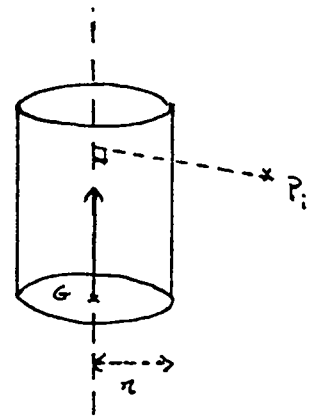

Fig. 2: Choice of the notations

---

minimize the energy:

$$E(x,y,z,\alpha,\beta,r) = \sum_{i=1}^{n}(\|G\vec{P}_i \wedge \vec{d}\|^2 - r^2\|\vec{d}\|^2)^2 \quad (1)$$

where n is the number of vertices of the wrinkle mask, P_i a vertex of the mask, and $\wedge$ denotes cross product. E is related to the square of the sum of distances between points of the mask and cylinder. The function E is minimized using a conjugate gradient method, since ∇E is easily computed:

$$\frac{\partial E}{\partial x} = -4\sum_{i=1}^{n}(\|G\vec{P}_i \wedge \vec{d}\|^2 - r^2\|\vec{d}\|^2) < G\vec{P}_i \wedge \vec{d} \mid \vec{i} \wedge \vec{d} > \quad (2)$$

$$\frac{\partial E}{\partial y} = -4\sum_{i=1}^{n}(\|G\vec{P}_i \wedge \vec{d}\|^2 - r^2\|\vec{d}\|^2) < G\vec{P}_i \wedge \vec{d} \mid \vec{j} \wedge \vec{d} > \quad (3)$$

$$\frac{\partial E}{\partial z} = -4\sum_{i=1}^{n}(\|G\vec{P}_i \wedge \vec{d}\|^2 - r^2\|\vec{d}\|^2) < G\vec{P}_i \wedge \vec{d} \mid \vec{k} \wedge \vec{d} > \quad (4)$$

$$\frac{\partial E}{\partial \alpha} = 4\sum_{i=1}^{n}((\|G\vec{P}_i \wedge \vec{d}\|^2 - r^2\|\vec{d}\|^2))(< G\vec{P}_i \wedge \vec{d} \mid G\vec{P}_i \wedge \vec{i} > -r^2 < \vec{d} \mid \vec{i} >) \quad (5)$$

$$\frac{\partial E}{\partial \beta} = 4\sum_{i=1}^{n}((\|G\vec{P}_i \wedge \vec{d}\|^2 - r^2\|\vec{d}\|^2))(< G\vec{P}_i \wedge \vec{d} \mid G\vec{P}_i \wedge \vec{j} > -r^2 < \vec{d} \mid \vec{j} >) \quad (6)$$

$$\frac{\partial E}{\partial r} = -4\sum_{i=1}^{n}\|\vec{d}\|^2 r(\|G\vec{P}_i \wedge \vec{d}\|^2 - \|\vec{d}\|^2 r^2) \quad (7)$$

Results are shown in figures 3 and 4. Figure 5 shows the result of the flattening.

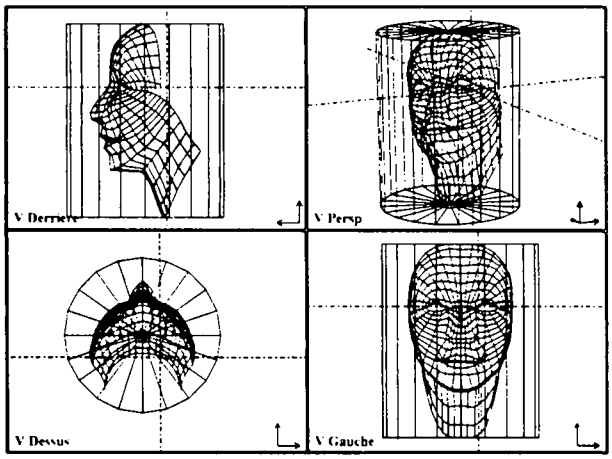

Fig. 3: Initial cylinder

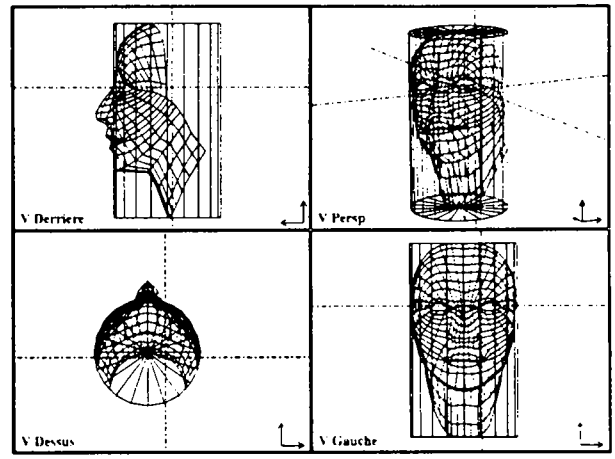

Fig. 4: Minimized cylinder

3.2 Adaptating the reference wrinkle mask to another face

The complete design of a wrinkle mask is a time consuming task since the user must draw the 0-isolines. Hence we need to develop tools permitting the mapping of the reference wrinkle mask onto another face. As mentioned before, the basic topology of the wrinkle mask is the same from one face to another; only the geometry and number of wrinkles vary. Let us consider the geometric data base of a new face. The new face is a 3D surface on which 0-isolines are not generally aligned with wrinkles (many devices for face acquisition just produce a polygonal approximation of a face). We define on this surface *characteristic geometric points*, such as the eye's ends, the border of the nose and chin, and the mask's boundary. The wrinkles and characteristic geometric points are cylindrically projected using the technique described before. We now have at our disposal the projected reference wrinkle mask, and the projected characteristics of the new one. The idea is then to move and fix projected reference characteristic points towards those of the new face. The projected reference wrinkles will be thus deformed by a dynamical system used to generate the new wrinkled face: a sprung mesh is generated in which the control points become the nodes of the mesh. Each connection becomes a spring of variable stiffness. The system runs according to the following dynamical equations:

$$m_i \vec{a_i} = \sum_{j=1}^{n(i)} k_{ij}(\|P_i\vec{P_j}\| - \|P_{0i}\vec{P}_{0j}\|)\frac{P_i\vec{P_j}}{\|P_i\vec{P_j}\|} - h\vec{v_i} \tag{8}$$

$i = 1, \ldots, N$, $j = 1, \ldots, n(i)$. The vector $\vec{a_i}$ is the acceleration vector of node i, $\vec{v_i}$ its velocity, m_i its mass; k_{ij} is the stiffness of spring $P_i\vec{P_j}$. The total number of nodes is N and $n(i)$ is the number of points connected with node i in the mesh. Finally, $\|P_{0i}\vec{P}_{0j}\|$ is the length of segment P_iP_j on the reference mask, $\|P_i\vec{P_j}\|$ the corresponding length on the new one, and h is the coefficient of velocity-dependent damping. Characteristic geometric points are kept fixed. After the new mask is

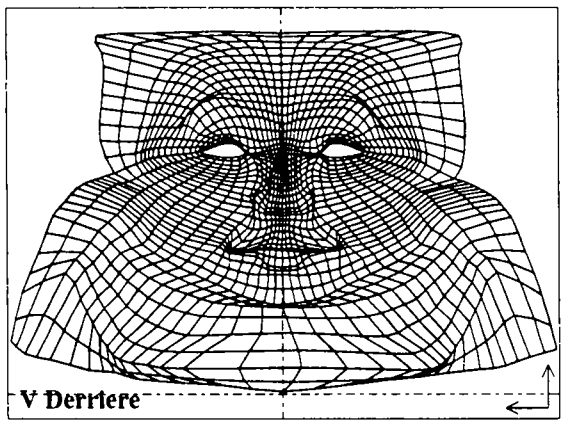

Fig. 5: Original flattened mask with characteristic geometric points moved

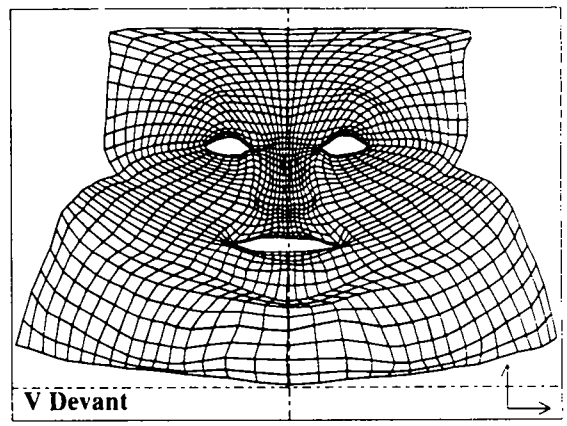

Fig. 6: Relaxed mask

relaxed, we project it back onto the surface of the new face, whose wrinkles are now aligned with the 0-isolines. If the user is not be entirely satisfied with the result (due to intrinsic limitations of such a spring-based dynamical system), he may move some points over the 3D surface, and rerun the relaxation.

Figure 5 shows the flattened mask before deformation. Figure 6 shows the result of the deformation, and in figure 7 we project the flattened mask back into 3D.

4 Facial animation

Muscle actions are modeled using force fields applied over *sprung objects* . Forces are associated with a button box and the deformations are generated in real time. We currently use eight types of forces or groups of forces to model 28 facial actions. The following muscles are taken into account: *masseter , frontal muscle, glabella depressor, eyebrow wrinkler, sphincter muscle of the eye (two actions), nasal muscle, upper lip and nasal wing elevator, upper lip elevator, lesser and greater zygomatic muscles, levator of the angle of the mouth, chin muscle, sphincter muscle of the mouth.*

The equation of the dynamics for a particular node i of the mesh is

$$m_i\vec{a_i} = \sum_{j=1}^{n(i)} k_{ij}(\|P_i\vec{P_j}\| - \|P_{0i}\vec{P}_{0j}\|)\frac{P_i\vec{P_j}}{\|P_i\vec{P_j}\|} - h\vec{v_i} + \sum \vec{F_{ext}} + \vec{F_r} \quad (9)$$

with the same notation as before, $\vec{F_{ext}}$ being the sum of the external forces acting on node i, and $\vec{F_r}$ the feedback force relative to the rest position: $\vec{F_r} = k\vec{P_iP_0}$.

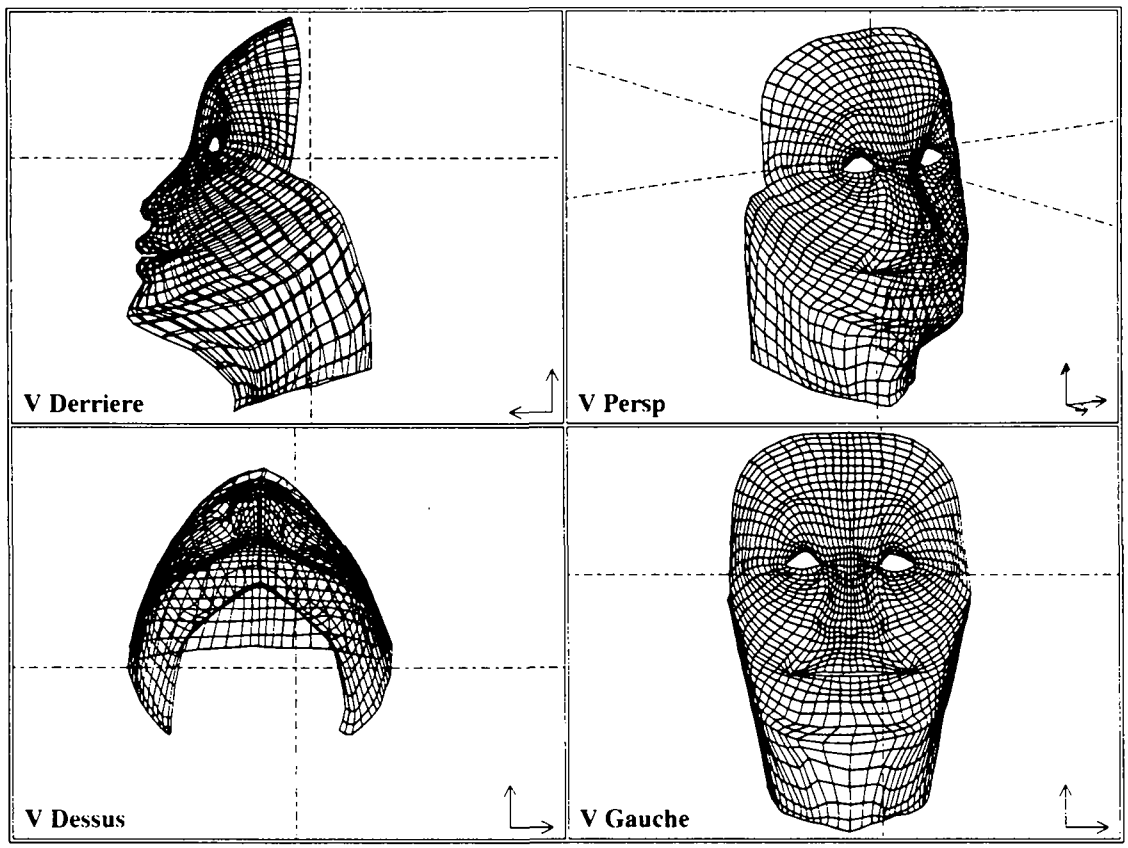

Fig. 7: Projection back to another face

Besides modeling, the user is provided with an animation system in which he can interactively define and modify 2D graphs denoting the variation in time of the amplitudes of the forces.

5 Modelisation of the bulge of the wrinkle

We now address the problem of modeling the wrinkle's bulge, then combine this model with the animation system of forces described in the preceding section.

As seen in section 2, the skin is made haggard by the action of time. Skin tissue changes due to two phenomenons: dilatation and changes in elasticity. To anticipate the generation of the bulge in the static case, it is the distension which create the bulge.

To understand that, let's draw a transversal cut of a piece of wrinkled skin (figure 8) and its development over time. We get a spline segment $C(u)$ such that $C(0) = P_0$, $C(1) = P_1$. Let's introduce a modulus of maximum dilatation DIL_{MAX} corresponding to the dilatation at maximum age AGE_{MAX}. We suppose the dilatation appears at age AGE_0 (35 years old approx.) and proceeds

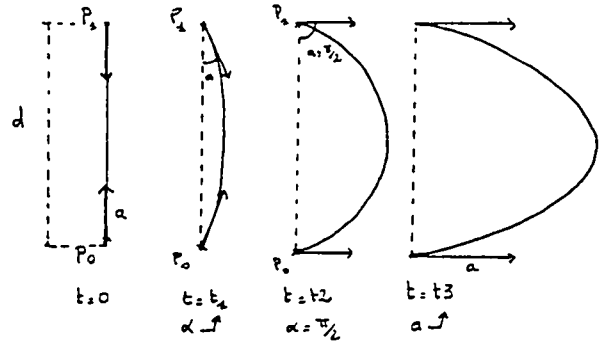

Fig. 8: 2D modeling of the bulge effect

linearly from AGE_0. Hence the arc-length of spline $C(u)$ at time t is

$$d_{real} = dil(d_{init}, t) = d_{init} max(1, (1 + (t - AGE_0)\frac{DIL_{MAX}}{AGE_{MAX} - AGE_0})) \tag{10}$$

Then the problem is well formulated: given $C(0)$ and $C(1)$, we look for the tangents $C'(0)$ and $C'(1)$ such that the arc-length of spline segment $C(u)$ is $d_{real} = dil(d_{init}, t)$. In order that the problem have a unique solution (modulo symmetry relative to segment P_0P_1) we add the following hypothesis: $C(u)$ is planar and symmetric relative to the median line of segment P_0P_1.

5.1 The 2D problem

What are the most important parameters for our problem ? We observe that wrinkles are not re-entrant rolls, but like low-relief, the maximum angle of the tangent of the roll relative to the reference tangent plane is $\leq \frac{\pi}{2}$ (figure 8). If the angle reaches the value $\frac{\pi}{2}$ and the target arc-length is not yet attained, we would like the roll to bulge more, thus increasing the tangent's amplitude. We conclude that the relevant parameters for the description of $C'(0)$ and $C'(1)$ are the angle α of the tangent relative to the reference plane and the norm a of the tangent.

We note that the problem is invariant by translation or rotation, but not by scaling. To simplify we take $P_0 = \begin{pmatrix} 0 \\ 0 \end{pmatrix}$ and $P_1 = \begin{pmatrix} d \\ 0 \end{pmatrix}$ and define control points P'_0 and P'_1 by

$$P'_0 = \begin{pmatrix} a\cos(\alpha) \\ a\sin(\alpha) \end{pmatrix} \tag{11}$$

$$P'_1 = \begin{pmatrix} d - a\cos(\alpha) \\ a\sin(\alpha) \end{pmatrix} \tag{12}$$

Let $S(d, a, \alpha)$ be the arc-length of the C-spline segment $\mathcal{C}$ passing through control points P_0, P_1 with tangents $P_0\vec{P'}_0$ and $P_1\vec{P'}_1$:

$$S(d, a, \alpha) = \int_0^1 \sqrt{\frac{dC_x}{du}(d, a, \alpha, u)^2 + \frac{dC_y}{du}(d, a, \alpha, u)^2}\, du \tag{13}$$

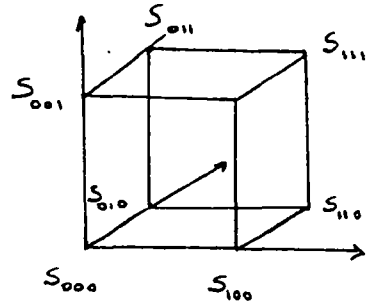

Fig. 9: Trilinear interpolation in a cube

C_x and C_y are the components of C. S is a function of three variables, so we choose to tabulate S: d varies from 0.1 to 20.1 by unit steps; a varies from 0 to 10 by unit steps; and α varies from 0 to $\frac{\pi}{2}$ by steps of size $\frac{\pi}{20}$.Desired values are obtained by trilinear interpolation over that domain.

In a small cube we get (see figure 9)

$$S(d,a,\alpha) = \sum_{i\in\{0,1\}} \sum_{j\in\{0,1\}} \sum_{k\in\{0,1\}} S_{ijk}((1-d)\delta_{i0} + d\delta_{i1})((1-a)\delta_{j0} + a\delta_{j1})((1-\alpha)\delta_{k0} + \alpha\delta_{k1}) \quad (14)$$

where δ_{ij} equals 1 when $i = j$, 0 if $i \neq j$. Knowing d, a and d_{real}, one seeks $S(d,a,\frac{\pi}{2})$. If the value obtained is greater than d_{real}, α is interpolated such that $S(d,a,\alpha) = d_{real}$, otherwise a is interpolated such that $S(d,a,\frac{\pi}{2}) = d_{real}$.

5.2 The 3D problem

We consider two types of expressive wrinkles: symmetric wrinkles such as the frontal ones, and unsymmetrical wrinkles such as nasolabial furrows. We'd like to keep our preceding hypothesis about symmetric planar splines in order to quickly compute the bulges. Thus we suppose that the spline segment to bulge is planar. For that hypothesis to be reasonable one must sufficiently refine the 3D spline in such a way that normal planes containing moving tangents are close enough to be considered as identical.

In our face modeling, at specific locations where wrinkles are defined, these normal planes are close enough for the error in arc-length to be negligible. The hypothesis of symmetry, in the case of symmetrical wrinkles is correct as long as one chooses a sufficiently refined sprung object. Indeed, since tangents are defined by pairs of neighbouring points, the more uniform is the mesh, the more symmetrical are the tangents. (Regularity of the mesh is moreover a condition for an acceptable evolution of the sprung surface as forces are applied to it).

Now tangent planes to the surface at P_0 and P_1 are not aligned anymore. This implies that α no longer varies between 0 and $\frac{\pi}{2}$ but rather between α_{min} and α_{max} with $\alpha_{max} = \alpha_{min} + \frac{\pi}{2}$ [†]. d remains $\|\vec{P_0P_1}\|$, but d_{init} corresponds to the arc length of the spline segment between P_0 and P_1 at a given

[†]The previous discretization of S is updated: α now varies between 0 and π

age depending only on the underlying sprung object at rest. We then compute d_{real} using (10) and we compute a and α using the methodology described above. Lastly we get the bulge effect (in the case of symmetric wrinkles) by rotating the desired tangent through an angle α relative to the axis (in the tangent plane) perpendicular to that tangent. The amplitude is increased if $\alpha = \alpha_{max}$.

The case of non-symmetrical wrinkles is treated analogously, but with a tabulation of S more adapted to that case.

From a user point of view, we associate "age" functionality of a sprung surface with a button box of an Iris Silicon Graphics workstation. The age of the data base can then be changed interactively. This functionality creates more or less marked wrinkles according to the age of the face. In other respects it is possible to associate with each wrinkle a particular coefficient to emphasize a specific wrinkle. An age being specified, the muscular transformations can be run, automatically operating with wrinkles given tensions and compressions generated by the forces.

5.3 Combination of wrinkles and forces

Given the temporal animation graphs and the elasticity parameters of the skin, the geometry of a face is automatically re-computed at each frame, using the interpolation methodology described above. Results are shown on the rendered images at the end of the paper.

6 Conclusion

We have presented some tools permitting the generation and animation of 3D wrinkled faces. Wrinkles were modeled and animated using dedicated techniques. A special effort has been made to keep the system interactive: all the paramters of the system can be inherited and adapted (wrinkles and forces) from one face to another, hence greatly simplifying facial modeling and animation each time a new face is acquired. This approach permits the generation of more realistic and expressive faces and animations.

We are now working additional models for aging. Expressive wrinkles are not the only sign of age. The modeling of the face and the skin's texture also change. These phenomena are not yet taken into account.

7 Acknowledgements

The authors would like to thank the referees for their helpful remarks.

References

[Kl89] **J. Kleiser,** *A fast, Efficient, Accurate Way to Represent the Human Face.* ACM Siggraph'89 Courses Notes, Vol 22:"State of the Art in Facial Animation" pp 20-33

[Pa82] **F. I. Parke,** *Parameterized Models for Facial Animation.* IEEE CG and A 9, 2, November 1982 pp 61-68

[Pa74] **F. I. Parke,** *A Parametric Model for Human Faces.* Phd dissertation, University of Utah, 1974.

[LePa89] **J. P. Lewis, F. I. Parke,** *Automated Lip-Synch and Speech Synthesis for Character Animation.* ACM Siggraph'89 Courses Notes, Vol 22:"State of the Art in Facial Animation" pp 64-68

[Pa89] **F. I. Parke,** *Parameterized Models for Facial Animation - Revisited.* ACM Siggraph'89 Courses Notes, Vol 22:"State of the Art in Facial Animation" pp 43-56

[Di89] **S. DiPaola,** *Implementation and use of a 3D Parameterized Facial Modeling and Animation System.* ACM Siggraph'89 Courses Notes, Vol 22:"State of the Art in Facial Animation" pp 20-33

[Tha88] **N. Magnenat-Thalmann, E. Primeau, D. Thalmann,** *Abstract muscle action procedures for face animation.* The Visual Computer, Vol 3, 1988, pp 290-297

[PlaBa81] **S. M. Platt, N. I. Badler,** *Animating Facial Expressions.* Computer Graphics, Vol 15, 3, 1981, pp 245-252

[Wa87] **K. Waters,** *A Muscle Model for Animating Three-Dimensional Facial Expressions.* SIGGRAPH 87, Proc. of Computer Graphics, Vol 21, 4, July 1987, pp 17-24

[KuAr90] **T. Kurihara, K. Arai,** *A Transformation Method for Modeling and Animation of The Human Face from Photographs.* Personnal Communication

[NaHuRiDo90] **M. Nahas, H. Huitric, M. Rioux, J. Domey,** *Facial Image Synthesis using Texture Recording.* The Visual Computer, Vol 6, 6, 1990 pp337-343

[Wi90] **L. Williams,** *Performance Driven Facial Animation.* SIGGRAPH 90, Proc. of Computer Graphics, 19(4):235-242. 1990.

[RoDe91] **H. Rouviere, A. Delmas,** *Anatomie Humaine Volume 1: Tete et Cou.* Editions Masson, Paris, 1991

[Hj69] **C-H. Hjortsjo,** *Human Mimicry.* Studentlitteratur, Oslo, 1969

[Cl81] **J. H. Clark,** *Parametric Curves, Surfaces and Volumes in Computer Graphics and Computer-Aided Geometric Design.* Technical Report No. 221, November 1981, Computer Systems Laboratory, Departments of Electrical Engineering and Computer Science, Stanford University, Stanford, California 94305

Fig. 10: Neutral face

Fig. 11: Disgust

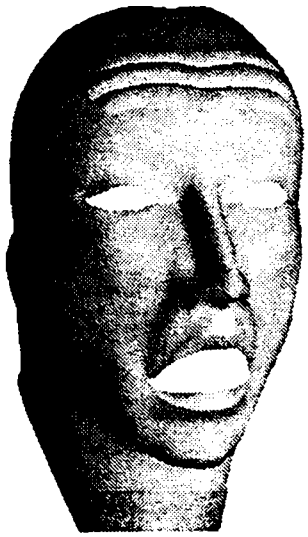

Fig. 12: Surprise

Fig. 13: Happiness 1

Fig. 14: Happiness 2

Fig. 15: Scepticism

Fig. 16: "... Really ? ..."

ISSN 0249-6399